Quaternary International 232 (2011) 122–131

Contents lists available at ScienceDirect

Quaternary International

journal homepage: www.elsevier.com/locate/quaint

Sea-level changes during the last 41,000 years in the outer shelf of the southern Tyrrhenian Sea: Evidence from benthic foraminifera and seismostratigraphic analysis

Antonio Caruso [a,*], Claudia Cosentino [a], Catherine Pierre [b], Attilio Sulli [a]

[a] Dipartimento di Geologia e Geodesia, Università degli Studi di Palermo, via Archirafi 20-22, 90123 Palermo, Italy
[b] UMR CNRS-UPMC-IRD 7159, LOCEAN, Université Pierre et Marie Curie, 4 Place Jussieu, 75252 Paris Cedex 05, France

ARTICLE INFO

Article history:
Available online 12 August 2010

ABSTRACT

An integrated high resolution study based both on a seismostratigraphic approach and on a sedimentary core (VIB 10), collected in the outer shelf (127 m depth) from the southern Tyrrhenian Sea (Gulf of Termini, Sicily), provides new data about climatic, eustatic and paleoenvironmental changes during the last ~41,000 years. The results based on the interpretation of a seismic profile, on benthic foraminifera assemblages and on $\delta^{18}O$ records, allowed recognition of two drastic sea-level falls during the Last Glacial Maximum (LGM) and the Younger Dryas (YD). The short deglacial event, between LGM and YD, known as Bølling/Allerød, played an important role in the sea-level rise that produced changes in benthic foraminiferal assemblages, favoring the proliferation of shallow water species of the inner shelf. After the Younger Dryas, warmer climatic conditions were rapidly established (Climatic Optimum) as indicated by the decrease of $\delta^{18}O$ values. The rapid sea-level rise due to the input of fresh water from ice caps melting following the increase of Earth's mean temperature is also indicated by the aggradational geometries of sedimentary layers observed in the seismic profile and by the increase of benthic foraminiferal species typical of the outer shelf.

1. Introduction

Global sea-level changes can be determined by several factors, including large-scale geological processes (plate tectonic movements which produce variations in the capacity of sedimentary basins), astronomical and sub-Milankovian cycles (Schulz, 2002; Caputo, 2007). Tectonic activity can also contribute to relative sea-level changes. As well, sedimentary inputs can influence relative sea-level changes, inducing lateral variations in coastal environments causing transgressive/regressive cycles (Trincardi and Field, 1991).

During the middle and the late Pleistocene, Milankovitch cycles induced climatic alternations of glacial and interglacial periods with the consequent expansion of the ice sheets and the cyclical abrupt fall of global temperatures and the sea-level, even if sub-Milankovian cycles also contributed to drastic short climatic changes (Schulz, 2002). During interglacial periods, the increase of global temperatures caused the ice caps to melt and consequentially the sea-level to rise.

The reconstruction of sea-level history through time can be carried out by using several sea-level markers, such as depositional indicators (analysis of notches, beach/lagoon, beach rocks, marine terraces transition deposits or backshore/foreshore deposits), erosional indicators (marine terraces or tidal notches) and biological indicators (i.e. lithophagus holes or coral reefs) (Bard et al., 1996; Antonioli et al., 1999), or submerged speleothems in coastal areas (Alessio et al., 1996; Antonioli et al., 2001), and submerged archaeological remains (Pirazzoli, 1976; Antonioli and Leoni, 1998). Furthermore, it is now established that oxygen isotope records of marine carbonate organisms represent a reliable tool for the reconstruction of relative variations of sea water temperature, as well as variations in ice volumes. Several authors have hypothesized that $\delta^{18}O$ fluctuations of 0.1‰ correspond to variations of about 10 m in the sea-level (Shackleton and Opdyke, 1973; Chappell and Shackleton, 1986; Hodell et al., 2002). Because local factors such as evaporation and dilution can interfere with the global isotopic signal, different conversion values were proposed (Fairbanks and Matthews, 1978; Labeyrie et al., 1987; Schrag et al., 1996; Waelbroek et al., 2002). Bintanja et al. (2005) concluded that

* Corresponding author. Tel.: +39 091 23864621; fax: +39 091 6169908.
E-mail address: acaruso@unipa.it (A. Caruso).

1040-6182/$ – see front matter © 2010 Elsevier Ltd and INQUA. All rights reserved.
doi:10.1016/j.quaint.2010.07.034

variations in the marine isotope $\delta^{18}O$ records cannot be linearly converted into sea-level changes (see a complete review in Caputo, 2007). According to Lambeck et al. (2004), sea-level is the sum of eustatic, glacio–hydro-isostatic, and tectonic factors.

The last ~41,000 years of Earth climate history have been characterized by an alteration of warm and cool periods; among these, the major abrupt cold events were the Last Glacial Maximum (26–19 ka) (Clark et al., 2009); and the Younger Dryas (~12,800–11,600 BP; Severinghaus et al., 1998; Stansell et al., 2010). Other shorter fluctuations towards cooler climatic conditions have been described, first in sediments from the North Atlantic, and are known as Heinrich events (Heinrich, 1988; Grousset et al., 1993; Bond et al., 1997; Hemming, 2004; Moreno et al., 2008). These climate events were also identified both in sedimentary marine cores from the Mediterranean basin (Cacho et al., 2001; Pérez-Folgado et al., 2003) and in Greenland ice cores (Dansgaard et al., 1993; Grootes et al., 1993). The warmest periods of the last ~41,000 years are known as Bølling–Allerød (~12,800–14,600 years ago) and Climatic Optimum, even if other minor warm shifts, followed by gradual cooling over a longer period when Dansgaard–Oeschger events (Dansgaard et al., 1993; Schulz, 2002) alternated with Heinrich events (Bond et al., 1997).

Since climatic reconstructions of the last 130 ka have become increasingly accurate, the recent literature has become richer and richer in studies focused on the reconstruction of sea-level curves by using different methodologies, such as high resolution seismostratigraphic analysis (i.e. Sacchi et al., 2009; Wright et al., 2009), the study of upper Quaternary terrace deposits (Nardin et al., 1981; Lambeck and Chappell, 2001), and radiometrically calibrated sediment cores from the Pacific Ocean (Bard et al., 1996), Red Sea (Siddall et al., 2003, 2009) and the central Indian Ocean (Kench et al., 2009).

In particular, Siddall et al. (2003) estimated important variations of the sea-level during the last 130 ka that were related to abrupt climate changes. These changes are generally induced by astronomical forcing, so that the highest rises occur in coincidence with

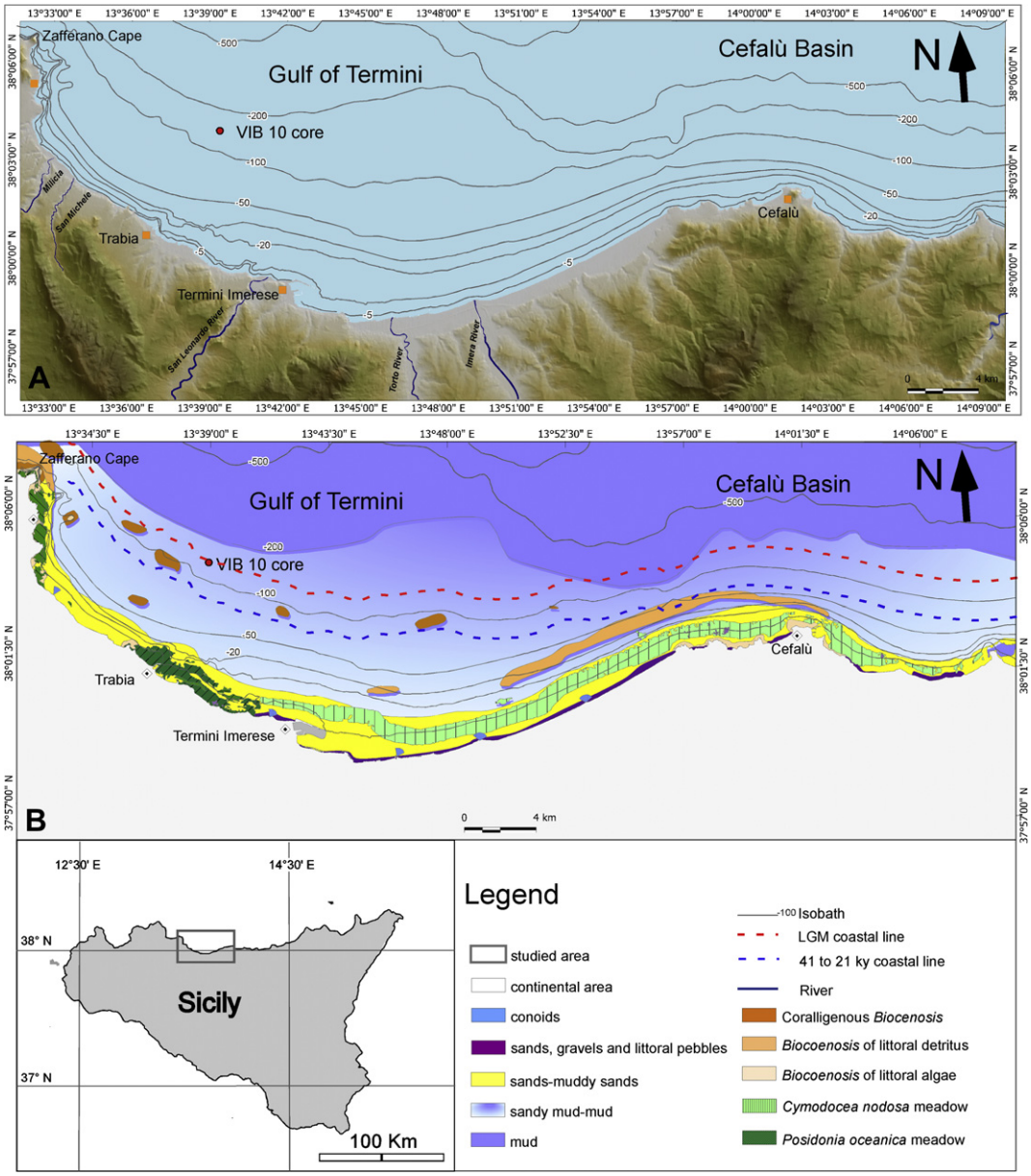

Fig. 1. Location map of the studied area; A) Corographic map of the Northern part of Sicilian coast and location of Vib 10 Core in the Gulf of Termini; B) Simplified skecth with sedimentological features and littoral biocoenocesis of the sea-floor (modified from CEOM, 2002).

insolation/eccentricity maxima, whereas sea-level falls coincide with insolation/eccentricity minima (see Shackleton, 1987, 2000). According to Wright et al. (2009), at ~35 ka along the New Jersey Margin, the sea-level was 60–80 m lower than today, with a major fall (−120 m) recorded between ~18 and 21 ka. From 18 ka the sea-level rose quickly because of the increase of Earth's mean temperature which caused the ice caps to melt (Siddall et al., 2003). Between ~18 and ~20 ka, Lambeck et al. (2011) estimated, along the northern part of Sicilian coast (Tyrrhenian Sea), a sea-level fall of 106 and 115 m, respectively. The authors proposed that after the LGM, between ~15,000 and 9000 years, the sea-level rose quickly. Unfortunately today no clear quantification exists about the sea-level variations during the Bølling–Allerød and the Younger Dryas periods.

For paleobathymetric reconstructions, micropaleontologists largely use benthic foraminifera because they provide environmental and ecological informations on the bottom waters (Murray, 1973; van der Zwaan et al., 1990; Jorissen et al., 1992; Scott et al., 2001; Kouwenhoven et al., 2003; van Hinsbergen et al., 2005). Each species prefers particular environmental conditions; for instance, *Ammonia* spp., *Elphidium* spp. and *Nonion* spp. prefer to live in the inner shelf. They are part of a genus that tolerate salinity variations well and are abundant in front of river mouths (Murray, 1973; Sgarrella and Moncharmont Zei, 1993; Sen Gupta, 1999). Epiphytic forms (i.e. *Asterigerinata* spp. and *Lobatula lobatula*) are abundant in the photic zone where coralligenous and seagrass biocoenosis are present (Langer, 1988; Sgarrella and Moncharmont Zei, 1993; Sen Gupta, 1999).

This article documents the climate and sea-level history of the last ~41,000 years in the southern Tyrrhenian Sea. This study is based on the reconstruction of a stratal pattern, as revealed by seismostratigraphic analysis, benthic foraminiferal assemblages and oxygen isotope records of benthic foraminifera.

2. Geological background

The sedimentary core was collected in the north Sicilian continental shelf (Fig. 1A), offshore Termini Imerese. The north Sicily continental margin (Gulf of Termini) occurs in the southern Tyrrhenian Sea, extending, from south to north, from the coastline of north Sicily to the Marsili Abyssal Plain (Pepe et al., 2005). The Gulf of Termini, 43 km in length, is bordered by the Zafferano Cape to the west and by the Cape of Cefalù to the east. *Posidonia oceanica* seagrass meadows are present along the inner shelf of the western and central part of the gulf (CEOM, 2002). Fig. 1B shows sedimentological features and a littoral biocoenosis of the sea-floor. The shelf is 2–8 km wide, with a slope gradient of about 1.5°. The depth of the shelf margin ranges from 120 to 135 m (Agate et al., 1998).

The sedimentary multilayer is composed by a middle Miocene to lower Pliocene tectonic edifice pertaining to the Sicilian segment of the Apenninic–Maghrebian chain, covered by less-deformed Neogene–Quaternary cover (Catalano et al., 1996). NW–SE- to E–W-trending normal faults, late Miocene in age, partially dissected the tectonic wedge to form extensional basins (such as the Cefalù Basin), filled by evaporitic, clastic and pelagic Messinian–Pleistocene deposits. Small-scale thrusting formed during the Middle Pliocene in the Cefalù Basin (Pepe et al., 2003), also responsible for the formation of minor intra-slope basins, while stretching mainly affected the margin during the middle–late Pliocene, causing normal faulting (Fabbri et al., 1981; Barone et al., 1982) and crustal thinning (Pepe et al., 2000). During the Pleistocene, E–W- to NE–SW-trending normal faults were quite common and exerted a control on the morphology of the shelf and coastal areas. Minor strike-slip Pliocene to Pleistocene structures are recognized in the eastern sector of the margin (Nigro and Sulli, 1995).

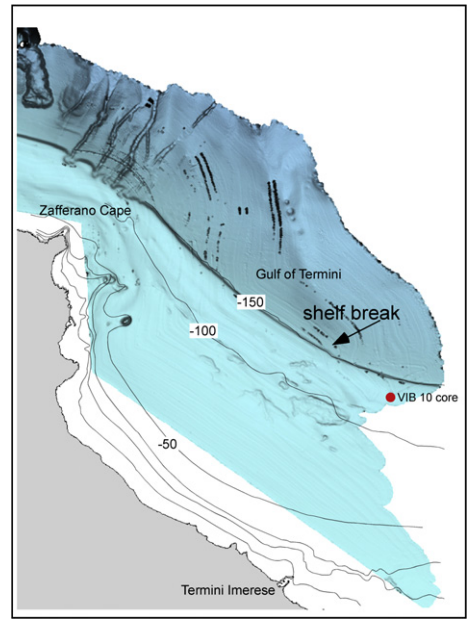

Fig. 2. Sea-floor topography illustrated by the MBES data. The VIB 10 core is located near the shelf margin.

In detail, the Quaternary deposits consist of clastic and terrigenous deposits over the shelf and the upper slope, whereas in the basinal areas hemipelagites are locally intercalated with volcanoclastic sediments (Pepe et al., 2003). The Quaternary succession in the shelf can be divided into depositional sequences of variable thickness and internal geometries bounded by unconformities. Their origin is related to Pleistocene–Holocene sea-level changes (Agate et al., 1993, 2005; Catalano et al., 1998), even if local uplift causes the systematic non-preservation of portions of the oldest sequences (Pepe et al., 2003).

3. Materials and methods

3.1. Multi-beam and seismic profile

The physiography of the area was depicted by means of Multi Beam Echo Sounder (MBES) data, acquired along the shelf to slope sector with a cell of 5 m. The processed data provided a high resolution three-dimensional image of the sea-floor (Fig. 2).

A set of single-channel seismic reflection profiles provided high resolution data of the sedimentary succession deeper than 200 m below the sea-floor. The seismic source was a multi-tip sparker array which provided high resolution data maintaining a good penetration. Processed seismic data was interpreted by using seismostratigraphic analysis, which allowed depositional units characterized by seismic facies with different attributes to be distinguished (Fig. 3).

3.2. Lithological description of the VIB 10 core

A sedimentary vibracore (VIB 10 Core, 353 cm in length) was collected in the outer shelf of the Gulf of Termini (Cefalù Basin) at a water depth of 127 m (38°03′57.7290 N; 13°39′57.8998 E) (Fig. 1). On the basis of lithological features, the core was subdivided into three different lithofacies (Fig. 4). In the first lithofacies (I), from the top to 180 cmbsf, sediments were mainly constituted of homogeneous yellowish mud. The second (II), from 180 to 233 cmbsf, was characterized by the presence of three sandy layers (a, b and c)

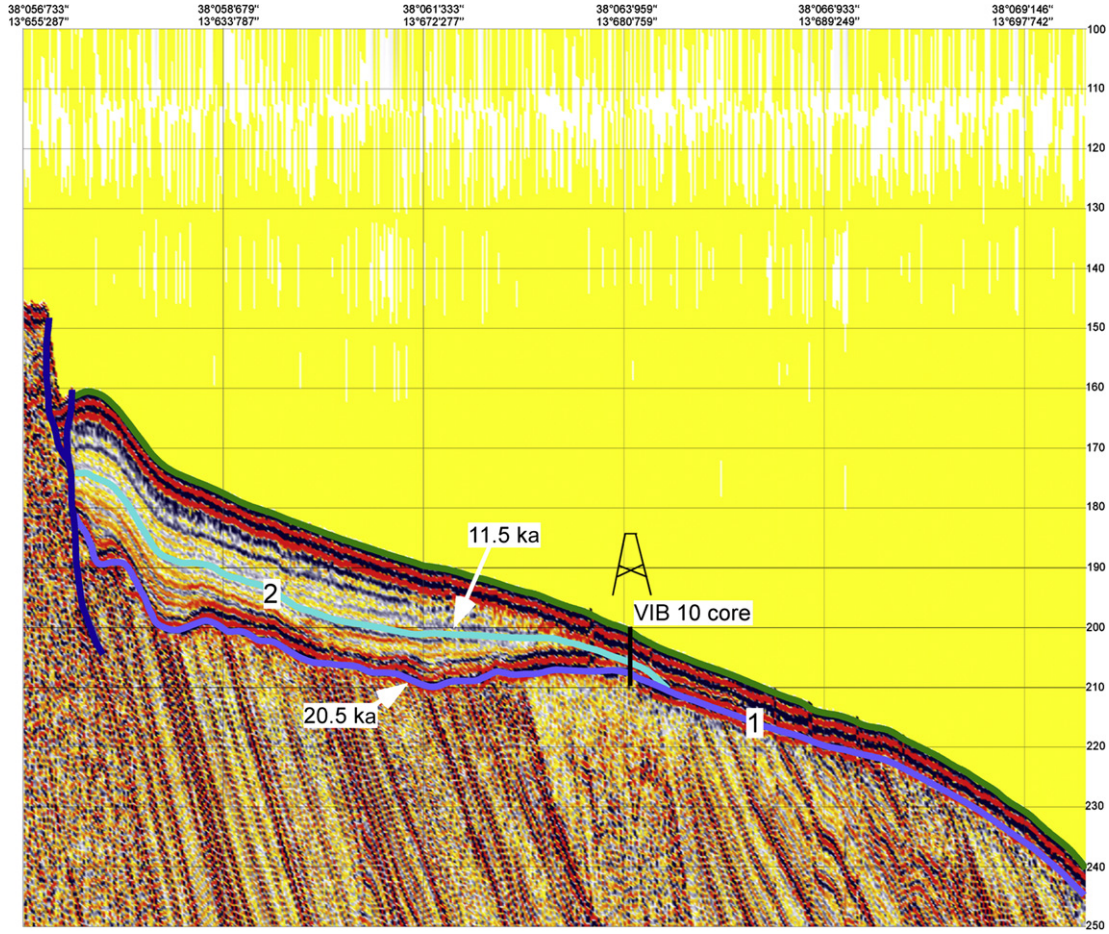

Fig. 3. High resolution seismic reflection profile pointing out the geometry of the Upper Pleistocene–Holocene depositional sequence. The arrows indicate the horizons correlated with the sea-level falls.

containing rounded grains and granules intercalated within grey mud. Layer "a", between 180 and 184 cmbsf, was rich in organogenic detritus, i.e. molluscs in their living position, fragments of echinoids and individual corals (genus *Flabellum*). Layers "b" and "c", between 202–216 and 228–233 cmbsf respectively, contained fragments of molluscs, echinoids and bryozoans; here, rounded grains and granules were common. The third lithofacies (III) of the core, from 233 to 353 cmbsf, was constituted of grey mud. For sampling, the core was sliced every 2 cm providing 174 samples that were studied for sedimentological, micropaleontological and isotopic analysis.

3.3. Granulometric and benthic foraminiferal analysis

For each sample, the wet sediment was oven-dried at 80 °C. The dried sediment was weighed and washed through a 63 μm sieve. The residual fraction was oven-dried again at 80 °C and weighed to obtain, by difference, the percentage of mud (silt + clay); on this fraction benthic foraminiferal analyses were carried out. The sediment was split into smaller aliquots, weighed, and all benthic foraminifera were identified and counted. Foraminiferal species were determined using the taxonomic classifications of AGIP (1982), Loeblich and Tappan (1988), Cimerman and Langer (1991), Sgarrella and Moncharmont Zei (1993). About 80 species were recognized, but here only a few species are discussed; they have been selected in relation to their specific environmental characteristics and according to the purpose of this study. To better show how benthic foraminifera can be used as proxies in the reconstruction of sea-level fluctuations (van Hinsbergen et al., 2005 and reference therein), percentages of abundance of species typical to the inner shelf were grouped (i.e. *Ammonia* spp., *Elphidium* spp., Miliolids, *L. lobatula*, *Hanzawaia boueana*, *Planorbulina acervalis*, *Asterigerinata* spp., *Rosalina* spp.), reported as "shallow water species". *Bolivina*, *Bulimina* and *Uvigerina* (Bul + Bol + Uvi) were also placed together, as they are generally abundant in the outer shelf. In the sandy layers (a, b and c) benthic foraminiferal tests were generally well preserved, even if in a few layers, a few individuals, belonging to *Adelosina* spp., showed pyritized and encrusted tests.

3.4. Benthic foraminiferal oxygen isotope records

Stable isotopic analyses were performed on the species *Melonis padanum*. For each sample, about 8–10 specimens were hand-picked from the fraction greater than 63 μm and analyzed on an ISOPRIME Dual Inlet Isotopic Ratio Mass Spectrometer at the Laboratoire d'Oceanographie et du Climat (LOCEAN) of the University Pierre and Marie Curie (Paris). Only 3–4 specimens were analyzed and, 40 samples were re-picked and re-analyzed in order to assess the reproducibility of the individual isotopic measurements. Oxygen isotope compositions are expressed in ‰ versus VPDB (Vienna Pee Dee Belemnite standard).

3.5. Radiocarbon dates and age model

The age model of the core was based on radiocarbon chronology (4 samples) and on oxygen isotope stratigraphy. Radiocarbon ages

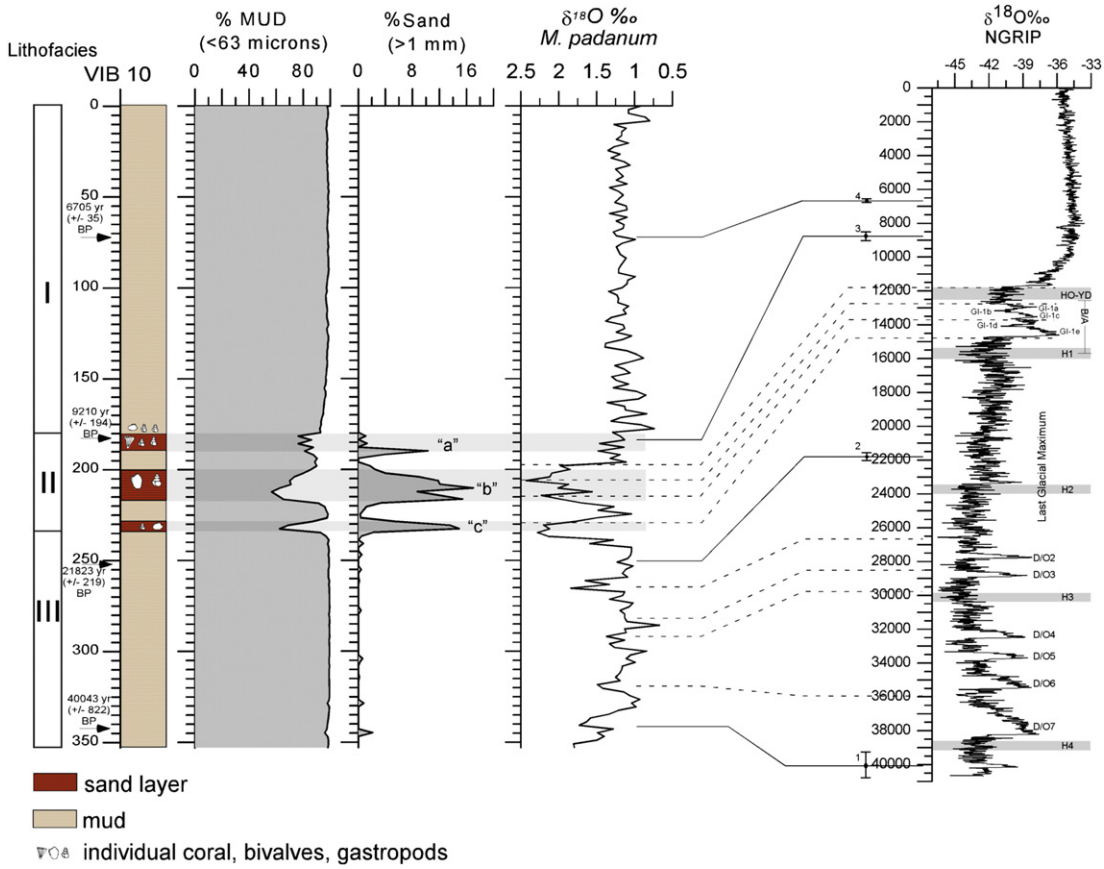

Fig. 4. Lithological log of VIB 10 sediment Core with mud and sand fraction percentages, $\delta^{18}O_{M.padanum}$ and $\delta^{18}O$ NGRIP isotope. To the left of the lithological log, calibrated radiocarbon ages are reported. Solid line correlation between radiometric ages, obtained for VIB 10 and NGRIP; Dotted line hypothesized correlation between $\delta^{18}O_{M.padanum}$ and $\delta^{18}O$ NGRIP (H = Heinrich events; B/A = Bølling/Allerød; YD = Younger Dryas; GI = Greenland Interstadial; D/O = Dansgaard/Oeschger).

for 3 samples were determined through the accelerator mass spectrometry (AMS) of benthic foraminiferal test at the Laboratoire de Mesure du Carbone CEA, Saclay (Paris). About 2–4 mg of dry samples were used for AMS measurements. Radiocarbon age for 1 sample was determined on an individual coral, by the conventional method using a liquid scintillation counter at LOCEAN (Paris) (Table 1). The Radiocarbon ages were calibrated to calendar years before the present (cal BP) using the software CALIB 6.0. (Stuiver et al., 2009), with Marine 09 dataset (Reimer et al., 2009); calibration used the maximum values exported by the CALIB program, and the 2-sigma error ranges along with the median ages from CALIB are reported in Table 1.

The chronology of the core was supplemented by identifying some well-dated climatic events by comparing the $\delta^{18}O$ curve with the $\delta^{18}O$ records of the NGRIP ice core, as for instance the Greenland Interstadial (GI) present in the Bølling–Allerød (B/A) period (Mangerud et al., 1974) and the Heinrich (H) and Dansgaard/Oeschger (D/O) events. The radiometric ages and other tie-points used for this study are reported in Table 1. The $\delta^{18}O_{M.padanum}$ fluctuations (Fig. 4) were correlated to the isotopic records of NGRIP (NGRIP Members, 2004) using calibrated radiocarbon ages as a tie-point, implemented with the ages of the climatic events (i.e. Younger Dryas, Bølling–Allerød, Heinrich). An age depth model was constructed using median calibrated radiocarbon ages (Fig. 5A)

Table 1
Radiocarbon ages of marine organisms used in study. Calibrated ages are in calendar years BP. Ages obtained with CALIB 6.0 are the median maximum likelihood values (parentheses). Other climatic events used for the reconstruction of the age depth model of VIB 10 core.

LAB Sample	Depth (cmbsf)	^{14}C AMS dating	Measured error (±)	2σ calibrated age (cal BP)	Datum
SacA 14312	70–72	6235	35	6683-(6705)-6728	Benthic foraminifera
Loc2009	182–184	8570	175	9006-(9210)-9414	individual coral (*Flabellum* sp.)
SacA 14311	250–252	18700	110	21605-(21823)-22042	Benthic foraminifera
SacA 14313	342–344	35380	710	39221-(40043)-40865	Benthic foraminifera

Depth (cmbsf) VIB 10	Other climatic Events	Calibrated Age (years)	References
180–182	top of younger Dryas	11,600	Stansell et al. (2010)
218–220	end of Bølling–Allerød	12,800	Stansell et al. (2010)
226–228	bottom of Bølling–Allerød	14,600	Stansell et al. (2010)
230–232	Henrich 1	~15,500	Cacho et al. (2001) – Mediterranean area
260–264	Henrich 2	~24,000	Cacho et al. (2001) – Mediterranean area
290–296	Henrich 3	~31,000	Cacho et al. (2001) – Mediterranean area
335–340	Henrich 4	~39,000	Cacho et al. (2001) – Mediterranean area

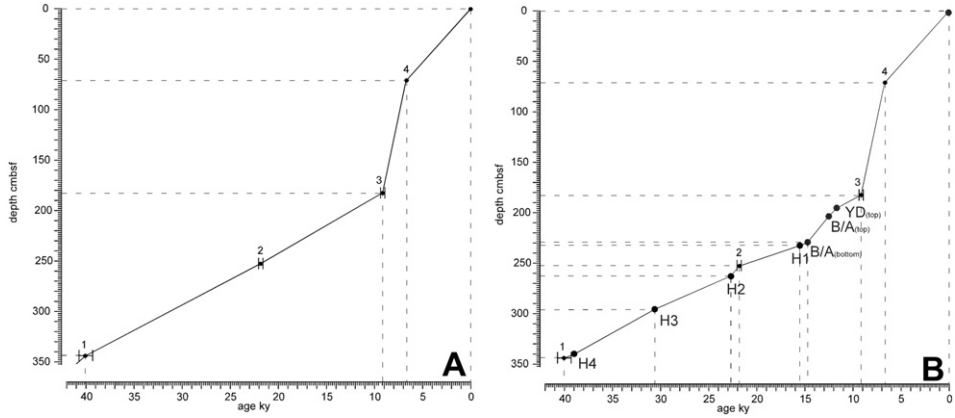

Fig. 5. A) Age depth model for the VIB 10 sediment Core obtained by using calibrated radiocarbon ages of individual coral and benthic foraminifera; B) Age depth model for the VIB 10 sediment core obtained by using calibrated radiocarbon ages and well-dated climatic events (H = Heinrich events; B/A = Bølling/Allerød; YD = Younger Dryas).

and another more accurate model was constructed using both YD, BA, and H events, and radiometric ages (Fig. 5B).

4. Results

4.1. Seismostratigraphy

In the drilled shelf area, the margin is located at about 150 m and the Lowstand Prograding Complex is absent, although it is widespread in adjacent areas. The shelf has a high gradient, which is interrupted by a step with a displacement of about 4 m located at a depth of about 100 m. This structure is interpreted as the result of a near-vertical fault.

The high resolution seismic profile (Fig. 3) demonstrates that the Pleistocene–Holocene sedimentary successions consist of: a) a group of Pleistocene strata that dip seaward and represent the prograding sequences accreting the continental shelf. These strata are topped by a widespread erosional truncation linked to the last (glacial) sea-level fall; b) Holocene mainly aggrading strata, lying on the erosional truncation, representing the Transgressive–Highstand Systems Tract of the last depositional sequence. These strata appear to be slightly deformed near to the sub-vertical fault described above. In this sector, the falling stage and low-sea-level deposits are nearly absent.

The age-dated core samples calibrated both the Upper Pleistocene deposits below the erosional truncation surface, and the Holocene deposits of the Transgressive–Highstand Systems Tract. Inside the latter is a horizon, at ~11.5 ka, which could be correlated with a minor sea-level fall, as demonstrated by the occurrence of sandy levels in the mainly marly deposits.

Retrogradational to aggradational geometries in the overlying deposits indicate that the transgressive to highstand systems tract, lying above an erosional truncation that could correspond to the ravinement surface, correlatable to the fossil-rich level in the Vib 10 core.

4.2. Lithology, isotopic analysis and benthic foraminifera of VIB 10 core

Sediments of lithofacies III (from ~41 to 20.8 ka) were mainly constituted by high percentages (93 and 98%) of mud fraction and large fluctuations of $\delta^{18}O_{M.padanum}$ were measured, with values

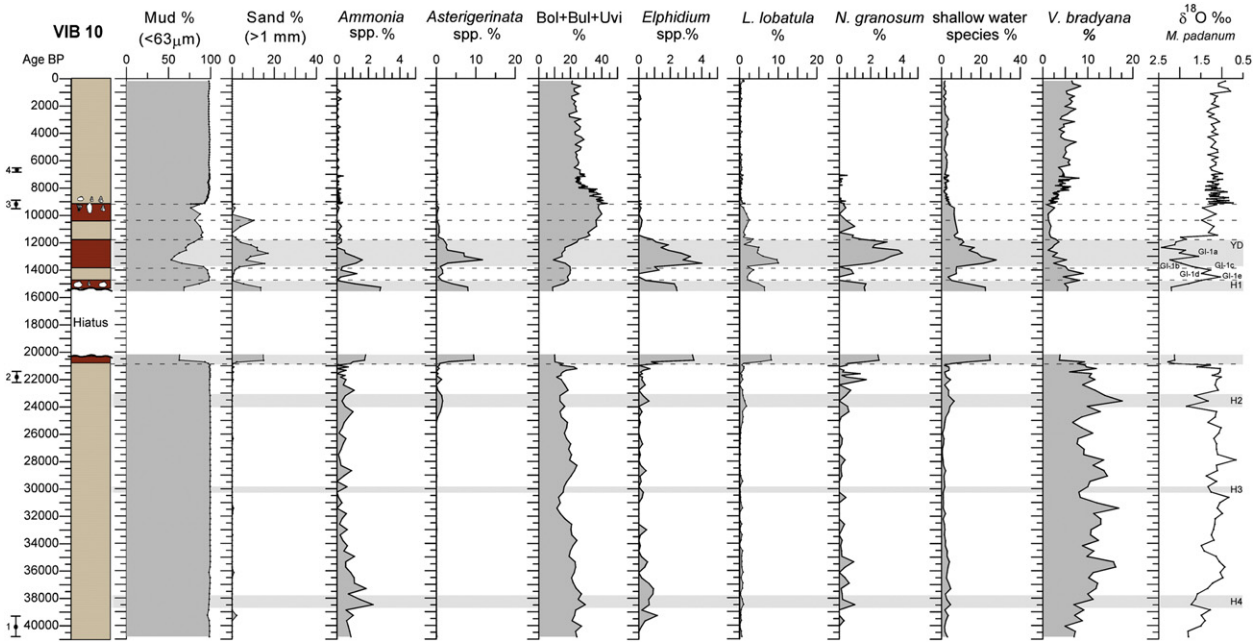

Fig. 6. Lithological log of VIB 10 Core in function of time, mud and sand fraction percentages, benthic foraminiferal curves and $\delta^{18}O_{M.padanum}$.

Table 2
Classification of the three lithofacies of VIB 10 sediment Core on the basis of sedimentological and micropaleontological features.

Lithofacies		Depth	Age	Depositional environment	Sediment composition	Other fragments	Benthic foraminifera
I		0–180 cmbsf	0–9.0 ky BP	outer shelf (95–120 m)	yellowish mud	–	*Bolivina* spp., *Bulimina* spp.
	a	180–190 cmbsf	9.0–10.5 ky BP	middle shelf (70–90 m)	grey sandy clays	individual corals, fragments of molluscs and echinoids	*Bolivina catanensis, Bulimina* spp.
II	**b**	200–216 cmbsf	12.0–13.3 ky BP	inner shelf (30–40 m)	organogenic detritus, grey sandy clays, rounded granules	rare fragments of molluscs and echinoids	*Asterigerinata* spp., *Ammonia* spp., *Elphidium* spp., *L. lobatula, N. granosum*
		228–232 cmbsf	14.2–15 ky BP	inner shelf (20–40 m)	grey sandy clays with rounded granules	rare fragments of molluscs and echinoids	*Asterigerinata* spp., *Ammonia* spp., *Elphidium* spp., *L. lobatula, N. granosum*
		230 cmbsf	15–20.5 ky BP	**EROSIONAL HIATUS**	**EROSIONAL HIATUS**	**EROSIONAL HIATUS**	**EROSIONAL HIATUS**
	c	230–232 cmbsf	15.5–20.5 ky BP	inner shelf (20–40 m)	grey sandy clays with rounded granules	rare fragments of molluscs and echinoids	*Asterigerinata* spp., *Ammonia* spp., *Elphidium* spp., *L. lobatula, N. granosum*
III		236–353 cmbsf	22.0–41 ky BP	middle shelf (60–80 m)	grey mud	–	*Bulimina* spp., *Bolivina* spp., *Uvigerina* spp.

ranging from 1.7 to 0.5‰. On the basis of the age model, high and low $\delta^{18}O_{M.padanum}$ values were correlated to cold and warm events of the $\delta^{18}O$ NGRIP record (Fig. 4). In lithofacies III benthic foraminiferal assemblages (Fig. 6 and Table 2) were dominated by significant abundances of *Bolivina, Bulimina, Uvigerina and Valvulineria bradyana*, while *Asterigerinata* was not present until ~25 ka and when present (from ~24.5 to ~20.8 ka) percentages of abundance were very low (max 2.5%). *L. lobatula*, *Elphidium* spp. and *Nonion granosum* were rare, with percentages ranging from 0 to 5% while *V. bradyana* showed a trend of increase (Fig. 6).

Sediments of lithofacies II covered the interval from ~20.6 to ~9 ka. This interval was characterized by the strongest variations in granulometry, with fluctuations of mud fraction from 53 to 98%. The sandy layers "a" and "b" were not generally considered as re-sedimented because some mollusks were in their living position, and no gradation was observed, even if some specimens of benthic foraminifera, found in the sandy layer "c", were probably displaced. Sandy layers "a", "b" and "c" were characterized by peaks of abundance of sands with high percentages of grains >1 mm (Figs. 4 and 6); The strongest $\delta^{18}O_{M.padanum}$ variations were recognized in coincidence with these layers, with values ranging from 2.4 to 1.4‰ (Fig. 4). Layers "b" and "c" were also characterized by the presence of several species typical of nearshore association such as *Ammonia* group, *Elphidium* group, *Asterigerinata* group, *L. lobatula*, *N. granosum*. Here, a drastic decrease of outer shelf species such as *Bolivina, Bulimina, Uvigerina and V. bradyana* was recognized; they showed an anti-correlative behavior with respect to the nearshore species.

The seismostratigraphic pattern, benthic assemblages and the age model indicate the presence of a hiatus from ~20.6 to ~15 ka in sandy layer "c".

Lithofacies I, from ~9 ka to the present, was characterized by the rapid increase of mud fraction (95–99%), while $\delta^{18}O_{M.padanum}$ displayed weak fluctuations between 1.4 and 0.6‰. This interval was also characterized by the drastic decrease, or disappearance, of the inner shelf species, i.e. *L. lobatula*, *Ammonia* group, *Elphidium* group and *N. granosum* and by the increase of *Bolivina*, *Bulimina*, *Uvigerina* and *V. bradyana* (Fig. 6 and Table 2).

5. Discussion

The studied core was subdivided into three lithofacies on the basis of the seismostratigraphic pattern, sedimentological features, benthic foraminiferal assemblages and $\delta^{18}O$ record of benthic foraminifera.

5.1. Lithofacies III (from ~41 to ~20.8 ka)

During this interval, the thin sedimentary layers showed an aggradational stratal pattern, with the characters of a condensed section that corresponds to the lower part of the VIB 10 core. This sedimentary body could correspond to the upper part of the interval included between the last depositional sequence and the upper part of the previous one. In particular, its geometry is typical of the falling stage systems tracts (Vail et al., 1991; Hunt and Tucker, 1992; Sacchi et al., 2009). This body was bounded at the top by an erosional truncation that corresponds to the ~20 to ~15 ka hiatus in the core. This erosional truncation (erosive regression) was caused by the sea-level fall of ~115 m at its maximum stage started during the Last Glacial Maximum. Moreover, the seismostratigraphic analysis allowed a reconstruction of the depositional events that characterized the studied area during the last ~41 ka, describing high frequency transgression–regression cycles. Sediments of this interval were characterized by high percentages of mud fraction and high percentages of abundance of benthic foraminifera. In particular, benthic foraminiferal assemblages were dominated by *Bolivina*, *Bulimina*, *Uvigerina* (Fig. 6), typical genera that prefer to live at depths deeper than 50–70 m. *V. bradyana* was also common with percentages of abundance between 8 and 20%, on the contrary, *Ammonia* and *Elphidium*, species that proliferate in shallow water environments and generally prefer to live between 0 and 80 m, with a maximum of abundance between 0 and 40 m (Sgarrella and Moncharmont Zei, 1993; Sen Gupta, 1999) were present with percentages >3%. Furthermore the *Ammonia* group is highly tolerant of rapid changes in water salinity and for this reason it can survive in estuarine environments. *Asterigerinata* and *L. lobatula* are typical of shallow water, but their abundance is above all linked to the presence of vegetation and coralligenous biocoenosis on the sea-floor. The low percentages of *Ammonia* and *Elphidium*, the contemporaneous presence of high percentages of *Bolivina*, *Bulimina* and *Uvigerina*, together with the absence of *L. lobatula* and *Asterigerinata* spp., suggest a paleodepth of 60–80 m, with strong inputs of continental fresh water (Fig. 7).

According to Cacho et al. (2001) between 41 and 21 ka in the western Mediterranean sea surface temperatures were cooler by 5–10° compared to today. In the Mediterranean area there is no palaeo sea-level curve during this interval (Lambeck et al., 2011). However, the situation was not very different from that in Red Sea where the sea-level was 60–80 m lower than today (Siddall et al., 2003). In the record, the lowest $\delta^{18}O_{M.padanum}$ values were similar

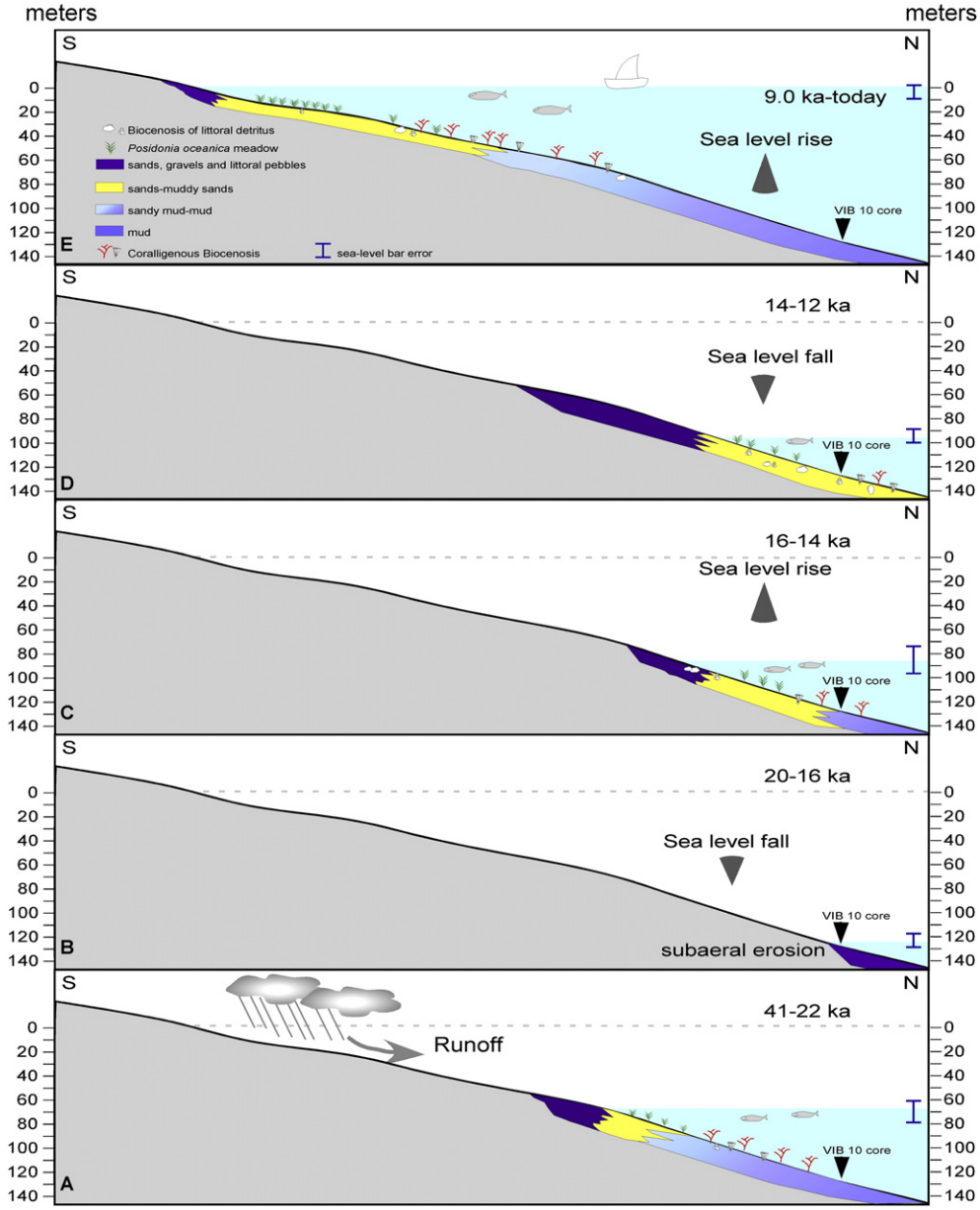

Fig. 7. Schematic profile (not to scale) from the North Sicilian coast of the Gulf of Termini seaward up to a depth of 150 m. Sea-level evolution during the last 41,000 years; between 41,000 and 22,000 years the sea-level was ~60–80 m less than today. The maximum fall occurred between 20,000 and 16,000 years. After the Younger Dryas the sea-level rose up quickly.

to those measured during the Climatic Optimum. The coastline was probably shifted 2–4 km seaward (Fig. 1) so that fresh water inputs from the five rivers arriving into the Gulf of Termini could have contributed to the decrease of $\delta^{18}O$ values of surface sea water. As the water depth at the site of the core Vib 10 would have been about 50–80 m, dilution was also affecting the bottom water. The lower $\delta^{18}O_{M.padanum}$ values have thus been correlated with the warm humid periods, labeled as Dansgaard/Oeschger events, alternating with cooler events, well identified in the NGRIP isotopic curve. This interval also included the H4, H3 and H2 events at ~39, ~30and ~24 ka, respectively.

5.2. Lithofacies II (from ~20.6 to ~9.0 ka)

During this interval the sedimentary succession lying above the erosional truncation showed an aggradational stratal pattern and can be interpreted as the transgressive systems tracts of the last depositional sequence. Here, the coastal facies progressively migrated landwards (transgression) (Figs. 3 and 7). This sedimentary body was bounded by a high amplitude reflector (see 2 in Fig. 3), correlable to the sandy layer "b" in the core, that corresponds to a minor sea-level fall during GI-1b and the Younger Dryas events. In this stage the coastal facies moved seawards (moderately erosive regression) (Fig. 7). This interval was characterized by the strongest variations both in the mud fraction, by the highest percentages of shallow water benthic foraminifera species and by large variations of the $\delta^{18}O_{M.padanum}$ values. The sandy layer "c" was considered as the sedimentary expression of the maximum sea-level fall due to the Last Glacial Maximum with an erosional surface between ~20.5 and ~15 ka (Figs. 6 and 7). In particular, *Ammonia*, *Nonion*, *Elphidium* and epiphytic forms become relatively abundant into the layer "c"; this sedimentological variation was well recognizable also by the increase of $\delta^{18}O_{M.padanum}$ values. The upper part of sandy layer "c" has been correlated to the H1 (Fig. 4).

From ~14.5 to ~12.8 ka, the shift of $\delta^{18}O_{M.padanum}$ values was attributed to the Bølling/Allerød period. This warming period, alternating with minor cool events, caused the ice sheet to melt and consequentially the sea-level to rise, indicated in the VIB 10 core by the increase of mud fraction, the decrease of shallow water benthic foraminifera species and the increase of *Bolivina*, *Bulimina* and *Uvigerina*. This change in benthic foraminiferal assemblages suggested a rapid rising of the sea-level of about 20–30 m. The coldest event (GI-1b), into the Allerød period, corresponds to an abrupt change in sedimentation rate with the deposition of the sandy layer "b" that persists up to the end of the Younger Dryas. During this short period, the percentage of sands increases up to 18–20%, together with shallow water benthic foraminifera species. Epiphytic forms, typical of 20–40 m depth, reached the highest percentage of abundance. Thus, the data indicated a sea-level fall of about 20–30 m during the GI-1b event, even if Lambeck et al. (2011) did not describe any sea-level fall during this period, along the northern part of the Sicilian coast.

5.3. Lithofacies I (from ~9.0 ka to today)

The seismostratigraphic pattern is characterized by an aggradational to retrogradational geometry that testifies the transgressive to highstand systems tracts, linked to the sea-level rise and to a landwards shift of the coastal facies (transgression) up to the present-day sea-level and coastal facies distribution. This interval is characterized by the stability of the $\delta^{18}O_{M.padanum}$ values and of the benthic foraminifera assemblages that were dominated by *Bolivina*, *Bulimina* and *Uvigerina*. The warming trend was due to the rapid increase of 8–10° of Earth's mean temperature (Siddall et al., 2003), also well indicated in the sea surface water of the Mediterranean basin (Cacho et al., 2001, 2002; Sbaffi et al., 2001; Kuhnt et al., 2007; Melki et al., 2009; Numberger et al., 2009), that caused the ice sheet melting and the consequent abrupt sea-level rise. According to Lambeck et al. (2011) from 11.5 to 9 ka the sea-level rose by 35 m.

The whole described sequence, shown in the seismic profile, is involved in a tectonic event caused by low-angled faults (Fig. 3). The displaced layers appear to be successively slightly deformed of ~10 m, that suggest sin–tectonic activity.

6. Conclusions

A micropaleontological and isotopic study performed on a sedimentary core collected in the continental shelf along the Sicilian coast has been compared with the seismostragraphic analysis of the studied area. It allowed reconstruction of the paleoenvironmental and the paleoclimatic history of the southern Tyrrhenian Sea during the last ~41 ka. In particular, lithological variations, drastic changes of the benthic foraminiferal assemblages and of the $\delta^{18}O_{M.padanum}$ values highlighted an alternation of warm and cold periods linked to eustatic fluctuations during the last climatic cycles.

All data support the identification of two abrupt sea-level falls; the first sea-level fall between ~20.5 and 15 ka produced a sea-level fall of ~115 m with the consequent subaerial exposure of the depositional site of VIB 10 core. During the second sea-level fall of ~20–30 m, the paleodepth of the depositional site of Vib 10 was 50–60 m; this fall started at ~14 ka, and was at maximum in coincidence of the cooling GI-1b at 13.4 ka. From 41 to 20.8 ka, the north Sicilian continental shelf underwent the influence of local factors, as inputs of fresh water from the continental area that modified the $\delta^{18}O_{M.padanum}$ values. These inputs were amplified by sea-level falls and by the migration of the coastline seawards so that river mouths were closer to the depositional site of the VIB 10 sediment core.

Acknowledgements

The authors are grateful to Arenaria S.p.a. that permitted the study of the VIB 10 Core. This study has been supported by Italian funds (A. Sulli) and by research grants from CNRS-LOCEAN (C. Pierre). We are also very grateful to Marie-José Urrutiaguer and Jérôme Demange for their technical assistance of isotopic analysis and Magloire Mandeng Yogo for Jean François Saliège (LOCEAN) for technical assistance for the radiometric ages. We thank Fabrizio Lirer and an anonymous reviewer for useful suggestions. We are also grateful to Cassandra Funsten who carefully reviewed the English.

References

Agate, M., Catalano, R., Infuso, S., Lucido, M., Mirabile, L., Sulli, A., 1993. Structural evolution of the northern Sicily continental margin during the Plio-Pleistocene. In: Max, M.D., Colantoni, P. (Eds.), Geological Development of the Sicilian-Tunisian Platform. Unesco Reports on Marine Science, vol. 58, pp. 25–30.

Agate, M., D'Argenio, A., Di Maio, D., Lo Iacono, C., Lucido, M., Mancuso, M., Scannavino, M., 1998. La dinamica sedimentaria dell'offshore della Sicilia nord-occidentale durante il tardo Quaternario. In: Catalano, R., Lo Cicero, G. (Eds.), Guida Escursioni 79° Congresso Nazionale Della Società Geologica Italiana. La Sicilia Occidentale, 1, pp. 157–167.

Agate, M., Mancuso, M., Lo Cicero, G., 2005. Late Quaternary sedimentary evolution of the Castellamare gulf (North-Western Sicily offshore). Bollettino Società Geologica Italiana 124, 21–40.

AGIP, 1982. Foraminiferi padani (Terziario e Quaternario). Atlante iconografico e distribuzione stratigrafica, second ed. AGIP Mineraria Milano, pp. 52.

Alessio, M., Allegri, L., Antonioli, F., Belluomini, G., Improta, S., Manfra, L., Preite, M., 1996. La curva di risalita del Mare Tirreno negli ultimi 43 ka ricavata da datazioni su speleotemi sommersi e dati archeologici. Memorie Descrittive del Servizio Geologico Nazionale 52, 235–256.

Antonioli, F., Leoni, G., 1998. Siti Archeologici e Loro Utilizzazione Quali Indicatori per lo Studio delle Variazioni Recenti del livello del Mare. Il Quaternario (Italian Journal of Quaternary Sciences), 122–139.

Antonioli, F., Silenzi, S., Frisia, S., 2001. Tyrrhenian Holocene palaeoclimate trends from speleanserpulids. Quaternary Science Reviews 20, 1661–1670.

Antonioli, F., Silenzi, S., Vittori, E., Villani, C., 1999. Sea level changes and tectonic stability: precise measurements in 3 coastlines of Italy considered stable during last 125 ky. Physics and Chemistry of the Earth 24, 337–342.

Bard, E., Hamelin, B., Arnold, M., Montaggioni, L., Gabioch, G., Faure, G., Rougerie, F., 1996. Deglacial sea-level record from Tahiti corals and the timing of global meltwater discharge. Nature 382, 241–244.

Barone, A., Fabbri, A., Rossi, S., Sartori, R., 1982. Geological structure and evolution of the marine areas adjacent to the Calabrian arc. Earth Evolution Science 3, 207–221.

Bintanja, R., van de Wal, R.S.W., Oerlemens, J., 2005. Modelled atmospheric temperatures and global sea levels over the past million years. Nature 437, 125–128.

Bond, G., Showers, W., Cheseby, M., Lotti, R., Almasi, P., deMenocaul, P., Priore, P., Cullen, H., Hajdas, I., Bonani, G., 1997. A pervasive millennial-scale cycle in North Atlantic Holocene and glacial climates. Science 278, 1257–1265.

Cacho, I., Grimalt, J.O., Canals, M., 2002. Response of the Western Mediterranean Sea to rapid climatic variability during the last 50,000 years: a molecular biomarker approach. Journal of Marine Systems 33–34, 253–272.

Cacho, I., Grimalt, J.O., Canals, M., Sbaffi, L., Shackleton, N.J., Schönfeld, J., Zahn, R., 2001. Variability of the Western Mediterranean Sea surface temperature during the last 30,000 years and its connection with the northern hemisphere climatic changes. Paleoceanography 16, 40–52.

Caputo, R., 2007. Sea-level curves: perplexities of an end-user in morphotectonic applications. Global and Planetary Change 57, 417–423.

Catalano, R., Di Stefano, P., Sulli, A., Vitale, F.P., 1996. Paleogeography and structure of the Central Mediterranean: sicily and its offshore area. Tectonophysics 260, 291–323.

Catalano, R., Di Stefano, E., Sulli, A., Vitale, F.P., Infuso, S., Vail, P.R., 1998. Sequences and systems tracts calibrated by high-resolution bio-chronostratigraphy: the central Mediterranean Plio-Pleistocene record. SEPM Special Publication 60, 115–177.

CEOM, S.C.p.A., 2002. Mappatura delle praterie di Posidonia oceanica lungo le coste della Sicilia e delle isole minori circostanti. Rapporto tecnico. Ministero dell'Ambiente e del Territorio, 644 pp.

Chappell, J., Shackleton, N.J., 1986. Oxygen isotopes and sea level. Nature 324, 137–140.

Cimerman, F., Langer, M.R., 1991. Mediterranean foraminifera. Academia Scientiarum et Artium Slovenica, Ljubljana 30, 1–118.

Clark, P.U., Dyke, A.S., Shakun, J.D., Carlson, A.E., Clark, J., Wohlfarth, B., Mitrovica, J.X., Hostetler, S.W., McCabe, A.M., 2009. The last glacial maximum. Science 325, 710–714.

Dansgaard, W., Johnsen, S.J., Clausen, H.B., Dahl-Jensen, D., Gundestrup, N.S., Hammer, C.U., Hvidberg, C.S., Steffensen, J.P., Sveinbjornsdottir, A.E., Jouzel, J.,

Bond, G., 1993. Evidence for general instability of past climate from a 250-ka ice-core record. Nature 364, 218–220.
Fabbri, A., Gallignani, P., Zitellini, N., 1981. Geological Evolution of the Peri-Tyrrhenian Sedimentary Basins. In: Wezel, F.C. (Ed.), Sedimentary Basins of Mediterranean Margins. Tecnoprint, Bologna, pp. 101–126.
Fairbanks, R.G., Matthews, R.K., 1978. The marine oxygen isotope record in Pleistocene coral, Barbados, West Indies. Quaternary Research 10, 181–196.
Grootes, P.M., Stuiver, M., White, J.W.C., Johnsen, S., Jouzel, J., 1993. Comparison of oxygen isotope records from the GISP2 and GRIP Greenland ice cores. Nature 366, 552–554.
Grousset, F.E., Labeyrie, L., Sinko, J.A., Cremer, M., Bond, G., Duprat, J., Cortijo, E., Huon, S., 1993. Patterns of ice-rafted detrius in the glacial North Atlantic (40–55°N). Paleoceanography 8, 175–192.
Heinrich, H., 1988. Origin and consequences of cyclic ice rafting in the Northeast Atlantic Ocean during the past 130,000 years. Quaternary Research 29, 142–152.
Hemming, S.R., 2004. Heinrich events: massive late Pleistocene detritus layers of the North Atlantic and their global climate imprint. Reviews of Geophysics 42, RG1005.
Hodell, D.A., Charles, C.D., Curtis, J.H., Mortyn, P.G., Ninnemann, U.S., Venz, K.A., 2002. Data report oxygen isotope stratigraphy of ODP LEG 177 sites 1088, 1089, 1090, 1093 and 1094. In: Gersonde, R., Hodell, D.A., Blum, P. (Eds.), Proceedings of the Ocean Drilling Program, Scientific Results, vol. 177, pp. 1–26.
Hunt, D., Tucker, M.E., 1992. Stranded parasequences and the forced regressive wedge systems tract: deposition during base-level fall. Sedimentary Geology 81, 1–9.
Jorissen, F.J., Barmawidjaja, D.M., Puskaric, S., Van der Zwaan, G.J., 1992. Vertical distribution of benthic foraminifera in the northern Adriatic Sea: the relation with the organic flux. Marine Micropaleontology 19, 131–146.
Kench, P.S., Smithers, S.G., McLean, R.F., Nichol, S.L., 2009. Holocene reef growth in the Maldives: evidence of a mid-Holocene sea-level highstand in the central Indian Ocean. Geology 37 (5), 455–458.
Kouwenhoven, T.J., Hilgen, F.J., van der Zwaan, G.J., 2003. Late Tortonian-early Messinian stepwise disruption of the Mediterranean-Atlantic connections: constraints from benthic foraminiferal and geochemical data. Palaeogeography, Palaeoclimatology, Palaeoecology 198, 303–319.
Kuhnt, T., Schmiedl, G., Ehrmann, W., Hamann, Y., Hemleben, C., 2007. Deep-sea ecosystem variability of the Aegean Sea during the past 22 kyr as revealed by benthic foraminifera. Marine Micropaleontology 64, 147–162.
Labeyrie, L.D., Duplessy, J.C., Blanc, P.L., 1987. Variations in mode of formation and temperature of oceanic deep waters over the past 125,000 years. Nature 327, 477–481.
Lambeck, K., Antonioli, F., Anzidei, M., Ferranti, L., Leoni, G., Scicchitano, G., Silenzi, S., 2011. Sea level change along Italian coast during Holocene and projections for the future. Quaternary International 232, 250–257.
Lambeck, K., Antonioli, F., Purcell, A., Silenzi, S., 2004. Sea-level change along the Italian coast for the past 10,000 yr. Quaternary Science Reviews 23, 1567–1598.
Lambeck, K., Chappell, J., 2001. Sea level change through the last glacial cycle. Science 292, 679–686.
Langer, M., 1988. Recent epiphytic foraminifera from Vulcano (Mediterranean Sea). Révue de Paléobiologie Spéciale 2, 827–832.
Loeblich, A.R., Tappan Jr., H., 1988. Foraminiferal Genera and Their Classification, vol. 4. Van Nostrand Reinhold, New York.
Mangerud, J., Andersen, S.T., Berglund, B.E., Donner, J.J., 1974. Quaternary stratigraphy of Norden: a proposal for terminology and classification. Boreas 3, 109–128.
Melki, T., Kallel, N., Jorissen, F.J., Guichard, F., Dennielou, B., Berné, S., Labeyrie, L., Fontugne, M., 2009. Abrupt climate change, sea surface salinity and paleoproductivity in the western Mediterranean Sea (Gulf of Lion) during the last 28 kyr. Palaeogeography, Palaeoclimatology, Palaeoecology 279, 96–113.
Moreno, G.J., Fawcett, P.J., Anderson, R.S., 2008. Millennial- and centennial-scale vegetation and climate changes during the late Pleistocene and Holocene from northern New Mexico (USA). Quaternary Science Reviews 27, 1442–1452.
Murray, J.W., 1973. Distribution and Ecology of Living Benthic Foraminiferids. Heinemann Educational Books, London, p. 274.
Nardin, T.R., Osborne, R.H., Bottjer, D.J., Scheidemann, R.C., 1981. Holocene sea-level curves for Santa Monica shelf, California continental Borderland. Science 213, 331–333.
Nigro, F., Sulli, A., 1995. Plio-Pleistocene extensional tectonics in the Western Peloritani area and its offshore (northeastern Sicily). Tectonophysics 252, 295–305.
North Greenland Ice Core Project Members (NGRIP), 2004. High-resolution record of Northern Hemisphere climate extending into the last interglacial period. Nature 431, 147–151.
Numberger, L., Hemleben, C., Hoffmann, R., Mackensen, A., Schulz, H., Wunderlich, J.M., Kucera, M., 2009. Habitats, abundance patterns and isotopic signals of morphotypes of the planktonic foraminifer *Globigerinoides ruber* (d'Orbigny) in the eastern Mediterranean Sea since the Marine Isotopic Stage 12. Marine Micropaleontology 73, 90–104.
Pepe, F., Bertotti, G., Cella, F., Marsella, E., 2000. Rifted margin formation in the South Tyrrhenian Sea: a high-resolution seismic profile across the North Sicily passive continental margin. Tectonics 19, 241–257.
Pepe, F., Sulli, A., Agate, M., Di Maio, M., Kok, A., Lo Iacono, C., Catalano, R., 2003. Plio-Pleistocene geological evolution of the northern Sicily continental margin (southern Tyrrhenian Sea): new insights from high-resolution, multi-electrode sparker profiles. Geo-Marine Letters 23, 53–63.
Pepe, F., Sulli, A., Bertotti, G., Catalano, R., 2005. Structural highs formation and their relationship to sedimentary basins in the north Sicily continental margin (southern Tyrrhenian Sea): implication for the Drepano Thrust Front. Tectonophysics 409, 1–18.
Pérez-Folgado, M., Sierro, F.J., Flores, J.A., Cacho, I., Grimalt, J.O., Zahn, R., Shackleton, N., 2003. Western Mediterranean Planktonic foraminifera events and millennial climatic variability during the last 70 ka. Marine Micropaleontology 48, 49–70.
Pirazzoli, P.A., 1976. Sea level variations in the northwestern Mediterranean during roman times. Science 194, 519–521.
Reimer, P.J., Baillie, M.G.L., Bard, E., Bayliss, A., Beck, J.W., Blackwell, P.G., Bronk Ramsey, C., Buck, C.E., Burr, G.S., Edwards, R.L., Friedrich, M., Grootes, P.M., Guilderson, T.P., Hajdas, I., Heaton, T.J., Hogg, A.G., Hughen, K.A., Kaiser, K.F., Kromer, B., McCormac, F.G., Manning, S.W., Reimer, R.W., Richards, D.A., Southon, J.R., Talamo, S., Turney, C.S.M., van der Plicht, J., Weyhenmeyer, C.E., 2009. IntCal09 and Marine 09 radiocarbon age calibration curves, 0–50.000 years cal BP. Radiocarbon 51, 1111–1150.
Sacchi, M., Molisso, F., Violante, C., Esposito, E., Insinga, D., Lubritto, C., Porfido, S., Toth, T., 2009. Insights into flood-dominated fan deltas: very high-resolution seismic examples off the Amalfi cliffed coasts, eastern Tyrrhenian Sea. Geological Society 322, 33–71.
Sbaffi, L., Wezel, F.C., Kallel, N., Paterne, M., Cacho, I., Ziveri, P., Shackleton, N., 2001. Response of the pelagic environment to palaeoclimatic changes in the central Mediterranean Sea during the Late Quaternary. Marine Geology 178, 39–62.
Schrag, D.P., Hampt, G., Murray, D.W., 1996. Pore fluid constraints on the temperature and oxygen isotopic composition of the glacial ocean. Science 272, 1930–1932.
Schulz, M., 2002. On the 1470-year pacing of Dansgaard-Oeschger warm events. Paleocenography 17 (4), 1–10.
Scott, D.B., Medioli, F.S., Schafer, C.T., 2001. Monitoring in Coastal Environments Using Foraminifera and Thecamoebian Indicators. Cambridge University Press, p. 177.
Sen Gupta, B.K., 1999. Foraminifera in marginal marine environments. In: Sen Gupta, B.K. (Ed.), Modern Foraminifera. Kluwer Academic Publisher, Great Britain, pp. 141–159.
Severinghaus, J.P., Sowers, T., Brook, E.J., Alley, R.B., Bender, M.L., 1998. Timing of abrupt climate change at the end of the Younger Dryas interval from thermally fractionated gases in polar ice. Nature 391, 141–146.
Sgarrella, F., Moncharmont Zei, M., 1993. Benthic foraminifera of the gulf of Naples (Italy): systematics and autoecology. Bollettino Della Società Paleontologica Italiana 32 (2), 145–264.
Shackleton, N.J., 1987. Oxygen isotopes, ice volume and sea level. Quaternary Science Review 6, 183–190.
Shackleton, N.J., 2000. The 100,000-year Ice-age cycle identified and found to lag temperature, carbon dioxide, and orbital eccentricity. Science 289, 1897–1902.
Shackleton, N.J., Opdyke, 1973. Oxygen isotope and paleomagnetic stratigraphy of equatorial Pacific core V28-238: oxygen isotope temperatures and ice volume on a 105 and 106 year scale. Quaternary Research 3, 39–55.
Siddall, M., Rohling, E.J., Almogi-Labin, A., Hemleben, Ch., Meischner, D., Schmelzer, I., Smeed, D.A., 2003. Sea level fluctuations during the last glacial cycle. Nature 423, 853–858.
Siddall, M., Stocker, T.F., Clark, P.U., 2009. Constraints on future sea-level rise from past sea-level change. Nature Geoscience 2, 571–575.
Stansell, N.D., Abbott, M.B., Rull, V., Rodbell, D.T., Bezada, M., Montoya, E., 2010. Abrupt younger Dryas cooling in the northern tropics recorded in lake sediments from the Venezuela Andes. Earth and Planetary Science Letters 293, 154–163.
Stuiver, M., Reimer, P.J., Reimer, R.W., 2009. CALIB 6.0 (www program and documentation). http://calib.qub.ac.uk/calib/maual/ (Last accessed March 2010).
Trincardi, F., Field, M.E., 1991. Geometry, lateral variations, and preservation of downlapping regressive shelf deposits: eastern Tyrrhenian sea margin, Italy. Journal of Sedimentary Petrology 61, 775–790.
Vail, P.R., Audermad, F., Bowman, S.A., Eisner, P., Perez Cruz, G., 1991. The stratigraphic signature of tectonics, eustasy and sedimentation: an overview. In: Enseile, G., Ricken, A., Seilacker, A. (Eds.), Cycles and Events in Stratigraphy. Springer Verlag, New York, pp. 617–659.
van der Zwaan, G.J., Jorissen, F.J., De Stigter, H.C., 1990. The depth dependency of planktonic/benthic foraminiferal ratios: constraints and applications. Marine Geology 95, 1–16.
van Hinsbergen, D.J.J., Kouwenhovenb, T.J., van der Zwaan, G.J., 2005. Paleobathymetry in the backstripping procedure: correction for oxygenation effects on depth estimates. Palaeogeography, Palaeoclimatology, Palaeoecology 221, 245–265.
Waelbroek, C., Labeyrie, L., Michel, E., Duplessy, J.C., McManus, J.F., Lambeck, K., Balbon, E., Labracherie, M., 2002. Sea-level and deep water temperature changes derived from benthic foraminifera isotopic records. Quaternary Science Review 21, 295–305.
Wright, J.D., Sheridan, R.E., Miller, K.G., Uptegrove, J., Cramer, B.S., Browning, J.V., 2009. Late Pleistocene Sea level on the New Jersey Margin: implications to eustasy and deep-sea temperature. Global and Planetary Change 66, 93–99.